

in their study is shown in Figure 6.<sup>13</sup> A "cis-to-cis" rearrangement like that shown in Figure 5 can occur in either of the two planes that contain a heteroatom, the metal, and the vacant site, as is also shown in Figure 6. These cis-to-cis rearrangements would scramble the labeled carbonyl but would never allow direct trans incorporation. Our calculations indicate that this process has a very small energy barrier.

### Conclusion

From the calculations presented here, one may conclude that both ground-state and relaxation effects are important in cis labilization. Relaxation effects are more important for those heteroligands that are not merely weaker  $\pi$  acceptors but are  $\pi$  donors. In the fragments  $M(\text{CO})_4\text{L}$ , direct trans-vacancy to cis-vacancy conversion is a higher energy process than simple trans loss for thermal dissociation of CO from  $M(\text{CO})_5\text{L}$ . If a ligand that is more labile than CO is dissociated from the trans position, then a trans-vacancy to cis-vacancy conversion is possible but has

a calculated barrier for small L (in the gas phase) of about 10 kcal/mol. Indirect trans incorporation via a mechanism similar to that of Lichtenberger and Brown<sup>9</sup> is predicted to be a very low energy process and should be observed in multiple substitution processes.

**Acknowledgment.** We thank the National Science Foundation (Grant No. CHE 86-19420) and the Robert A. Welch Foundation (Grant No. A-648) for support of this work. This research was conducted in part by using the Cornell National Supercomputer Facility, a resource for the Center for Theory and Simulation in Science and Engineering at Cornell University, which is funded in part by the National Science Foundation, New York State, and the IBM Corp. We gratefully acknowledge the financial support by the Board of Regents, Texas A&M University, and a generous grant of computer time by Cray Research, Mendota Heights, MN.

**Registry No.**  $\text{Mn}(\text{CO})_5\text{Cl}$ , 14100-30-2;  $\text{Mn}(\text{CO})_5\text{H}$ , 16972-33-1;  $\text{Cr}(\text{CO})_5\text{Ph}_3$ , 18116-53-5;  $\text{Cr}(\text{CO})_5\text{NH}_3$ , 15228-27-0.

Contribution from the Departments of Medicinal Chemistry, Biomolecular Discovery, and Physical and Structural Chemistry, Smith Kline & French Laboratories, P.O. Box 1539, King of Prussia, Pennsylvania 19406-2799, and Department of Chemistry, Northeastern University, Boston, Massachusetts 02115

## $[\mu\text{-}1,1'\text{-Bis}(\text{diphenylphosphino})\text{ferrocene}]_{\text{bis}}(\text{chlorogold})$ : Synthesis, Iron-57 and Gold-197 Mössbauer Spectroscopy, X-ray Crystal Structure, and Antitumor Activity

David T. Hill,\*† Gerald R. Girard,† Francis L. McCabe,† Randall K. Johnson,† Paul D. Stupik,‡  
Jian H. Zhang,‡ William M. Reiff,‡ and Drake S. Eggleston§

Received August 8, 1988

The title compound **2**,  $\text{Fdpp}(\text{AuCl})_2$ , synthesized via the addition of **1** to an aqueous solution of  $[(\text{HOCH}_2\text{CH}_2)_2\text{S}]\text{AuCl}$  generated in situ by the thiodiglycol reduction of  $\text{HAuCl}_4$  showed a  $^{31}\text{P}\{\text{H}\}$  NMR chemical shift at  $\delta$  27.39, which was downfield from that of **1** at  $\delta$  -17.34 relative to  $(\text{CH}_3\text{O})_3\text{PO}$ . The  $^{57}\text{Fe}$  Mössbauer spectrum of **2** is a doublet with parameters (IS = 0.50 mm/s relative to Fe, QS = 2.33 mm/s) similar to those of ferrocene. The  $^{197}\text{Au}$  Mössbauer spectrum of **2** is an asymmetric doublet (QS = 6.93 mm/s) with an IS of 3.81 mm/s relative to Au metal.  $\text{Fdpp}(\text{AuCl})_2$  crystallized in space group  $P\bar{1}$  with lattice constants  $a = 16.192$  (4) Å,  $b = 16.921$  (4) Å, and  $c = 10.878$  (5) Å with  $Z = 3$ . Two crystallographically independent molecules, A and B, were observed in the structure of **2** with a chloroform solvate molecule per 1.5 formula units of the gold complex. For A, the P atoms are  $180^\circ$  opposed and the rings exactly staggered, while in B the P atoms are  $150^\circ$  apart and the rings are partially staggered. The P-Au-Cl linkage is nearly linear, and the bond distances fall within normal ranges. Evaluation in an ip P388 leukemia mouse model showed **1** and **2** to have only marginal activity with an increased life span (ILS) relative to untreated controls of 30% at a maximally tolerated dose (MTD) of 231  $\mu\text{mol}/\text{kg}$  and 40% ILS at 4  $\mu\text{mol}/\text{kg}$ , respectively.

### Introduction

The antitumor activity of bis(diphenylphosphines) and their bis(gold(I)) complexes has been of recent interest.<sup>1,2</sup> The spacer connecting the phosphine moieties has been varied, and a number of ligands and their gold complexes have been prepared and evaluated in a P388 leukemia mouse model.<sup>1</sup> Although some of the ligands have significant activity in this model, the corresponding gold complexes appear to have increased potency on a molar basis. Maximal activity was found when the phosphines were bridged by cis-ethylene or ethane, e.g. 1,2-bis(diphenylphosphino)ethane (dppe). Recently, several ferrocenium salts have been reported to be active against Ehrlich ascites tumor, producing cure rates of 70–100% over a broad dose range.<sup>3,4</sup> In addition, these ferrocenium compounds inhibited several solid tumors including B<sub>16</sub> melanoma, colon 38 carcinoma, and Lewis lung carcinoma.<sup>5</sup> Together these findings suggested that the incorporation of the essential structural features of the bis(phosphinogold) complexes with a ferrocene might provide compounds with antitumor activity.

A ligand incorporating the necessary structural elements suitable as a gold(I) complexing agent is the readily available phosphinoferrrocene: 1,1'-bis(diphenylphosphino)ferrocene (**1**).<sup>6</sup> This bidentate ligand is capable of both bridging and chelation and can form complexes with ratios of metal atom to ligand of 1 or 2, behaving in a manner similar to that of dppe.<sup>7</sup> Complexes of **1** with a variety of metals including Co,<sup>7</sup> Ni,<sup>7</sup> Hg,<sup>8</sup> Mo,<sup>9</sup> W,<sup>9</sup> Pd,<sup>10</sup> Pt,<sup>11</sup> and Rh<sup>12</sup> have been described. Solutions of **1**

- Mirabelli, C. K.; Hill, D. T.; Faucette, L. F.; McCabe, F. L.; Girard, G. R.; Bryan, D. B.; Sutton, B. M.; Bartus, J. O.; Croke, S. T.; Johnson, R. K. *J. Med. Chem.* **1987**, *30*, 2181.
- Mirabelli, C. K.; Jensen, B. D.; Mattern, M. R.; Sung, C.-M.; Mong, S.-M.; Hill, D. T.; Dean, S. W.; Schein, P. S.; Johnson, R. K.; Croke, S. T. *Anti-Cancer Drug Des.* **1986**, *1*, 223.
- Kopf-Maier, P.; Kopf, H.; Neuse, E. W. *Angew. Chem., Int. Ed. Engl.* **1984**, *23*, 456.
- Kopf-Maier, P.; Kopf, H.; Neuse, E. W. *J. Cancer Res. Clin. Oncol.* **1984**, *108*, 336.
- Kopf-Maier, P.; Kopf, H. *Chem. Rev.* **1987**, *87*, 1137.
- Bishop, J. J.; Davison, A.; Katcher, M. L.; Lichtenberg, D. W.; Merrill, R. E.; Smart, J. C. *J. Organomet. Chem.* **1971**, *27*, 241.
- Rudie, A. W.; Lichtenberg, D. W.; Katcher, M. L.; Davison, A. *Inorg. Chem.* **1978**, *17*, 2859.
- Mann, K. R.; Morrison, W. H., Jr.; Hendricksen, D. N. *Inorg. Chem.* **1974**, *13*, 1180.
- Baker, P. K.; Fraser, S. G.; Harding, P. *Inorg. Chim. Acta* **1986**, *116*, L5.
- Hayashi, T.; Konishi, M.; Kumoda, M. *Tetrahedron Lett.* **1979**, 1871.
- Clemente, D. A.; Pilloni, G.; Corain, B.; Longato, B.; Tiripicchio-Camellini, M. *Inorg. Chim. Acta* **1986**, *115*, L9.

\* Department of Medicinal Chemistry, Smith Kline & French Laboratories.

† Department of Biomolecular Discovery, Smith Kline & French Laboratories.

‡ Department of Physical and Structural Chemistry, Smith Kline & French Laboratories.

§ Northeastern University.

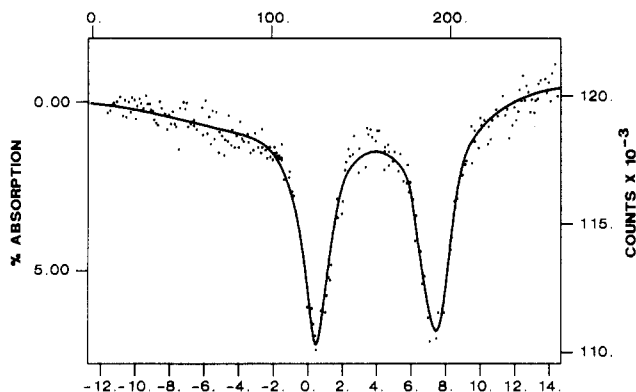


Figure 1.  $^{197}\text{Au}$  Mössbauer spectrum of  $\text{Fdpp}(\text{AuCl})_2$  (**2**) at 4.2 K.

and Rh have been investigated as catalysts in hydroformylation reactions with certain alkenes<sup>13,14</sup> as well as hydrogenation catalysts for olefins.<sup>12</sup> Despite the interest in metal coordination compounds of **1**, the gold complexes of Fdpp remain undescribed. Reported herein are the synthesis, iron-57 and gold-197 Mössbauer parameters, and X-ray crystal structure of  $\mu$ -[1,1'-bis(diphenylphosphino)ferrocene]bis(chlorogold), i.e.  $\text{Fdpp}(\text{AuCl})_2$  (**2**). The antitumor properties of **2** in a P388 leukemia mouse model are reported in comparison with the activity of the ligand **1**.

### Experimental Section

**Materials.** 1,1'-Bis(diphenylphosphino)ferrocene (Fdpp, **1**) was purchased from Strem Chemicals, Inc., P.O. Box 108, Newburyport, MA 01950.

**[ $\mu$ -1,1'-Bis(diphenylphosphino)ferrocene]bis(chlorogold) (**2**).** Thiodiglycol (2.0 g, 16.4 mmol) in methanol (10 mL) was added dropwise over 15 min to a solution of chloroauric acid tetrahydrate (1.5 g, 3.64 mmol) in water (10 mL)/methanol (50 mL) kept at 0 °C. After the solution was stirred an additional 15 min, Fdpp (**1**) (1.0 g, 1.82 mmol) in chloroform (75 mL)/methanol (30 mL) was added to the colorless solution with rapid stirring (immediate precipitate upon addition). The reaction mixture was stirred overnight, warming to room temperature. Methanol (200 mL) was added and the product collected and recrystallized from acetonitrile/methylene chloride to give 0.66 g of **2** as orange crystals. The filtrate was reduced in volume, ethanol added, and the resulting precipitate collected and recrystallized from acetonitrile/methylene chloride to give an additional 0.52 g of **2**. Total yield: 1.18 g (64%); mp 255 °C dec, uncor. Anal. Calcd for  $\text{C}_{34}\text{H}_{28}\text{Au}_2\text{Cl}_2\text{FeP}_2$ : C, 40.07; H, 2.77. Found: C, 40.16; H, 2.81.  $^1\text{H}$  NMR ( $\text{CDCl}_3$ ):  $\delta$  4.28 (mult, 4 H), 4.73 (mult, 4 H), 7.47 (mult, 20 H).  $^{31}\text{P}$  NMR ( $\text{CDCl}_3$ ):  $\delta$  27.39 (s).

**$^1\text{H}$  and  $^{31}\text{P}\{^1\text{H}\}$  NMR Spectra of Fdpp (**1**).**  $^1\text{H}$  NMR ( $\text{CDCl}_3$ ):  $\delta$  3.99 (mult, 4 H), 4.26 (mult, 4 H), 7.26 (mult, 20 H).  $^{31}\text{P}$  NMR ( $\text{CDCl}_3$ ):  $\delta$  -17.34 (s).

**Methods. NMR Spectra.** The  $^1\text{H}$  NMR spectra were obtained in  $\text{CDCl}_3$  by using a Bruker AM 250 spectrometer operating at 250 MHz and recorded at 297 K.  $^1\text{H}$  chemical shifts were relative to tetramethylsilane. The  $^{31}\text{P}\{^1\text{H}\}$  NMR spectra were recorded at 297 K by using a Bruker WM 360 spectrometer at 145.8 MHz. The  $^{31}\text{P}$  NMR samples were run in  $\text{CDCl}_3$  with  $(\text{CH}_3\text{O})_3\text{PO}$  ( $\delta(\text{P})$  2.0 ppm) in  $\text{CDCl}_3$  as the external standard.

**Mössbauer Spectrum.** The  $^{197}\text{Au}$  Mössbauer spectrum (Figure 1) was obtained on 100 mg of finely powdered crystals contained in a Nylon holder of 12-mm diameter. The holder was wrapped in aluminum foil and maintained at 4.2 K throughout the data collection. The instrumentation used was previously described,<sup>15,16</sup> and an integrating counting technique was used.<sup>17</sup> The recorded spectrum was fitted to a pair of Lorentzian lines,<sup>18</sup> and the isomer shift was measured relative to metallic

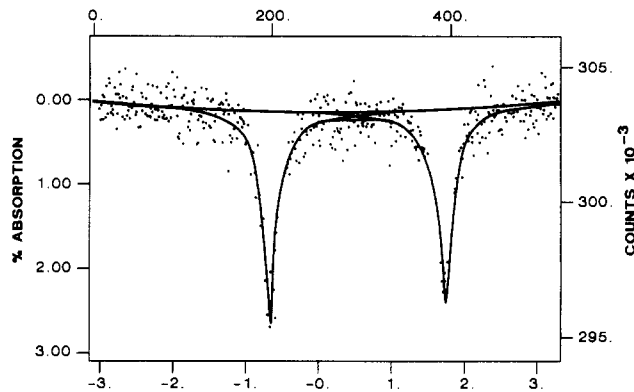


Figure 2.  $^{57}\text{Fe}$  Mössbauer spectrum of **2** at 49 K.

Table I. Crystal and Intensity Measurement Data for  $[\text{Fdpp}(\text{AuCl})_2]\cdot\text{CHCl}_3$

formula	$\text{Au}_2\text{Cl}_2\text{FeP}_2\text{C}_{34}\text{H}_{28}\cdot\text{CHCl}_3$
fw	1138.62
space group	$P\bar{1}$
$a$ , Å	16.192 (4) <sup>a</sup>
$b$ , Å	16.921 (4)
$c$ , Å	10.878 (5)
$\alpha$ , deg	93.09 (3)
$\beta$ , deg	94.28 (3)
$\gamma$ , deg	115.29 (2)
$V$ , Å <sup>3</sup>	2675.0 (33)
temp, K	293
$Z$	3
$\mu$ , cm <sup>-1</sup>	90.869
$D_x$ , g cm <sup>-3</sup>	2.120
$D_m$ , g cm <sup>-3</sup>	2.03 (1) ( $\text{CH}_2\text{Br}_2/\text{C}_3\text{H}_6\text{Br}_2$ )
cryst size, mm	0.30 × 0.30 × 0.05
radiation ( $\lambda$ , Å)	monochr Mo K $\alpha$ (0.71073)
instrument	CAD-4
scan type	$\omega$ - $\theta$
scan range ( $\Delta\omega$ ), deg	0.95 + 0.35 tan $\theta$
scan speed, deg min <sup>-1</sup>	variable, 3.5–10.5
max $2\theta$ , deg	50
reflens	0 ≤ $h$ ≤ 19, -19 ≤ $k$ ≤ 19, -12 ≤ $l$ ≤ 12
no. of measd reflens	9932
no. of reflens marked weak	1656
no. of unique reflens	8840
no. of "obsd" reflens, $I \geq 3\sigma(I)$	6346
merging $R$	0.022
params	592
agreement factors <sup>b</sup>	
$R$	0.042
$R_w$	0.053
$S$	1.17
transm coeff	max = 99.72% min = 30.26%

<sup>a</sup> A reduced triclinic cell is obtained if the transformation is made to  $a = 10.878$  Å,  $b = 16.19$  Å,  $c = 16.921$  Å,  $\alpha = 115.29^\circ$ ,  $\beta = 93.09^\circ$ , and  $\gamma = 94.28^\circ$ . <sup>b</sup> Agreement factors are defined as follows:  $R = \sum ||F_o| - |F_c|| / \sum |F_o|$ ;  $R_w = [\sum w(|F_o| - |F_c|)^2 / \sum w|F_o|^2]^{1/2}$ ;  $S = [\sum w - (|F_o| - |F_c|)^2 / N_o - N_v]^{1/2}$ . Weights:  $4(F_o)^2 / r^2(I)$  with  $\sigma(I) = [\sigma^2(I) + (0.05F_o)^2]^{1/2}$ .

gold foil. The  $^{57}\text{Fe}$  Mössbauer spectrum (Figure 2) was obtained at 50 K according to a previously published procedure.<sup>19</sup>

**Crystallographic Data Collection and Structure Determination for **2**.** Table I summarizes crystal and intensity measurement data. The orange crystals obtained on recrystallizing **2** from chloroform were prismatic needles. The crystal used for data collection was cleaved from a larger crystal to the dimensions stated (Table I). Unit cell dimensions were obtained from a least-squares fit of the setting angles for 25 reflections ( $30^\circ \leq 2\theta \leq 35^\circ$ ) on the diffractometer. Three reference reflections (876;  $\bar{1}$ 3,9,2; 12,9,1) were monitored every 3 h of exposure time; data were corrected for Lorentz-polarization factors, for a 1.5% deterioration in intensity, and for absorption. The absorption correction was based on  $\psi$  scans of nine reflections with  $80^\circ \leq \chi \leq 90^\circ$ . Positions of the gold

- (12) Cullen, W. R.; Kim, T.-J.; Einstein, F. W. B.; Jones, T. *Organometallics* **1985**, *4*, 346.  
 (13) Pittman, C. U., Jr.; Honnick, W. D.; Yang, J. J. *J. Org. Chem.* **1980**, *45*, 684.  
 (14) Pittman, C. U., Jr.; Honnick, W. D. *J. Org. Chem.* **1980**, *45*, 2132.  
 (15) Vieggers, M. P. A. Ph.D. Thesis, Catholic University of Nijmegen, Netherlands, 1976.  
 (16) Vieggers, M. P. A.; Trooster, J. M. *Phys. Rev. B: Solid State* **1977**, *15*, 72.  
 (17) Vieggers, M. P. A.; Trooster, J. M. *Nucl. Instrum. Methods* **1976**, *118*, 257.  
 (18) Hill, D. T.; Sutton, B. M.; Isab, A. A.; Razi, T.; Sadler, P. J.; Trooster, J. M.; Calis, G. H. M. *Inorg. Chem.* **1983**, *22*, 2936.

- (19) Cheng, C.; Reiff, W. M. *Inorg. Chem.* **1977**, *16*, 2097.

**Table II.** Positional Parameters and Their Estimated Standard Deviations

atom	x	y	z	$B^a$ Å <sup>2</sup>
Au1	0.13360 (3)	0.34156 (3)	0.14465 (4)	2.930 (9)
Au2	0.57291 (3)	0.16813 (3)	0.70630 (4)	3.77 (1)
Au3	0.12929 (3)	0.18837 (2)	0.28943 (4)	2.635 (8)
Fe1	0.000	0.500	0.000	2.72 (4)
Fe2	0.36020 (9)	0.17252 (9)	0.4813 (2)	3.28 (4)
Cl1	0.2790 (2)	0.3588 (2)	0.1124 (3)	4.79 (8)
Cl2	0.7173 (2)	0.2749 (3)	0.7009 (4)	6.4 (1)
Cl3	0.0430 (2)	0.0979 (2)	0.1191 (3)	4.53 (8)
Cl4	0.6952 (5)	0.4796 (5)	0.1851 (7)	13.6 (2)
Cl5	0.6538 (5)	0.3796 (5)	-0.0473 (7)	13.2 (3)
Cl6	0.5141 (5)	0.4046 (6)	0.067 (1)	21.7 (5)
P1	-0.0078 (2)	0.3300 (2)	0.1647 (2)	2.75 (6)
P2	0.4277 (2)	0.0694 (2)	0.7013 (3)	3.26 (6)
P3	0.2073 (2)	0.2629 (2)	0.4681 (3)	2.62 (6)
C1	-0.0498 (6)	0.2958 (6)	0.3118 (9)	2.9 (2)
C2	-0.0599 (7)	0.3527 (7)	0.399 (1)	4.0 (3)
C3	-0.0896 (8)	0.3260 (8)	0.512 (1)	5.0 (3)
C4	-0.1066 (8)	0.2436 (9)	0.540 (1)	5.3 (3)
C5	-0.0990 (8)	0.1841 (8)	0.455 (1)	4.7 (3)
C6	-0.0696 (7)	0.2107 (7)	0.339 (1)	3.5 (3)
C7	-0.0953 (6)	0.2496 (6)	0.0518 (9)	2.8 (2)
C8	-0.0676 (8)	0.2134 (7)	-0.048 (1)	4.2 (3)
C9	-0.1360 (9)	0.1523 (8)	-0.137 (1)	4.7 (3)
C10	-0.229 (1)	0.1313 (9)	-0.122 (1)	6.4 (4)
C11	-0.2535 (8)	0.1664 (8)	-0.026 (1)	4.5 (3)
C12	-0.1866 (8)	0.2264 (7)	0.061 (1)	4.2 (3)
C13	-0.0122 (7)	0.4335 (6)	0.1519 (8)	2.8 (2)
C14	-0.0903 (7)	0.4507 (7)	0.127 (1)	4.0 (2)
C15	-0.0560 (7)	0.5439 (6)	0.133 (1)	4.2 (2)
C16	0.0394 (9)	0.5831 (7)	0.159 (1)	4.6 (3)
C17	0.0671 (8)	0.5151 (7)	0.172 (1)	3.6 (3)
C18	0.1532 (6)	0.2099 (6)	0.5997 (9)	2.6 (2)
C19	0.0866 (7)	0.1254 (7)	0.5826 (9)	3.2 (3)
C20	0.0477 (8)	0.0811 (7)	0.684 (1)	4.4 (3)
C21	0.0763 (8)	0.1227 (9)	0.801 (1)	4.7 (3)
C22	0.1432 (8)	0.2087 (8)	0.821 (1)	4.9 (3)
C23	0.1811 (7)	0.2523 (7)	0.720 (1)	3.7 (3)
C24	0.2194 (7)	0.3742 (7)	0.488 (1)	3.5 (3)
C25	0.1543 (8)	0.3922 (7)	0.540 (1)	5.7 (3)
C26	0.1602 (9)	0.4780 (8)	0.547 (2)	6.5 (4)
C27	0.229 (1)	0.5412 (8)	0.497 (2)	6.8 (4)
C28	0.295 (1)	0.5241 (8)	0.441 (2)	7.0 (5)
C29	0.2909 (9)	0.4405 (8)	0.436 (1)	5.3 (4)
C30	0.3213 (7)	0.2729 (6)	0.488 (1)	3.4 (2)
C31	0.3762 (7)	0.2785 (7)	0.601 (1)	3.8 (3)
C32	0.4638 (8)	0.2872 (8)	0.570 (1)	4.6 (3)
C33	0.4640 (7)	0.2884 (7)	0.443 (1)	5.3 (3)
C34	0.3766 (7)	0.2781 (7)	0.387 (1)	4.4 (3)
C35	0.3640 (6)	0.0658 (6)	0.556 (1)	3.2 (2)
C36	0.2687 (7)	0.0555 (7)	0.539 (1)	4.2 (3)
C37	0.2498 (8)	0.0590 (8)	0.408 (1)	4.6 (3)
C38	0.3280 (8)	0.0695 (8)	0.352 (1)	4.7 (3)
C39	0.3975 (7)	0.0735 (7)	0.442 (1)	4.1 (3)
C40	0.3649 (6)	0.0883 (6)	0.822 (1)	3.3 (2)
C41	0.2831 (8)	0.0212 (8)	0.845 (1)	5.1 (3)
C42	0.2290 (9)	0.0352 (9)	0.933 (1)	6.4 (4)
C43	0.2662 (8)	0.1195 (9)	0.999 (1)	6.3 (4)
C44	0.3467 (9)	0.1859 (9)	0.976 (1)	6.8 (4)
C45	0.3975 (8)	0.1702 (8)	0.886 (1)	4.5 (3)
C46	0.4133 (6)	-0.0421 (7)	0.717 (1)	3.5 (2)
C47	0.3521 (8)	-0.1130 (7)	0.636 (1)	4.4 (3)
C48	0.3418 (9)	-0.1980 (8)	0.656 (2)	6.1 (4)
C49	0.3903 (9)	-0.2107 (7)	0.747 (1)	6.3 (3)
C50	0.451 (1)	-0.1422 (8)	0.830 (1)	7.5 (4)
C51	0.4653 (8)	-0.0539 (8)	0.814 (1)	5.3 (3)
C52	0.625 (1)	0.454 (1)	0.040 (2)	9.8 (7)

<sup>a</sup> $B^a$ 's for anisotropically refined atoms are given in the form of the isotropic equivalent displacement parameter defined as  $(4/3)[a^2B(1,1) + b^2B(2,2) + c^2B(3,3) + ab(\cos \gamma)B(1,2) + ac(\cos \beta)B(1,3) + bc(\cos \alpha)B(2,3)]$ .

atoms were deduced from a Patterson map; the remainder of the non-hydrogen atoms were located from difference Fourier synthesis. Difference maps also revealed the presence of a chloroform molecule, which was treated in subsequent refinement at full occupancy. All non-hy-

**Table III.** Principal Bond Distances (Å) and Angles (deg) for **2**

Bond Lengths			
Au1-Cl1	2.300 (3)	Au2-Cl2	2.273 (4)
Au1-P1	2.239 (3)	Au2-P2	2.222 (3)
P1-C1	1.81 (1)	Au3-Cl3	2.282 (3)
P1-C7	1.82 (1)	Au3-P3	2.229 (3)
P1-C13	1.79 (1)	P3-C18	1.82 (1)
P2-C35	1.81 (1)	P3-C24	1.82 (1)
P2-C40	1.82 (1)	P3-C30	1.79 (1)
Bond Angles			
Cl1-Au1-P1	176.0 (1)	Au2-P2-C40	114.8 (4)
Au1-P1-C1	114.8 (3)	Au2-P2-C46	114.3 (4)
Au1-P1-C7	112.9 (4)	Cl3-Au3-P3	173.4 (1)
Au1-P1-C13	111.2 (4)	Au3-P3-C18	112.1 (4)
Cl2-Au2-P2	175.5 (1)	Au3-P3-C24	114.2 (4)
Au2-P2-C35	110.5 (4)	Au3-P3-C30	113.2 (4)

drogen atoms were refined with anisotropic temperature factors. Final fractional atomic coordinates for non-hydrogen atoms may be found in Table II. Principal bond lengths and angles are compiled in Table III; the remainder of these metrical values have been deposited as supplementary material (Table SII). Anisotropic thermal parameters (Table SI), calculated hydrogen atom coordinates (Table SIII), and structure factors (Table SIV) have been included also as supplementary material.

### Results and Discussion

**Structural Data.** The title compound **2** was synthesized via addition of a solution of a stoichiometric amount of Fdpp (**1**) in chloroform/methanol to an aqueous solution of freshly prepared chloro(thiodiglycol)gold,  $[\text{HO}(\text{CH}_2)_2]_2\text{SAuCl}$  at 0 °C. The latter was formed in situ at 0 °C by reducing chloroauric acid in water with excess thiodiglycol. The resulting  $\text{Fdpp}(\text{AuCl})_2$  (**2**) precipitates from the reaction medium as it is formed and is easily isolated by filtration. Additional amounts of **2** were collected from the filtrate upon reduction in solvent volume. The complex **2** was obtained as orange crystals in 64% yield after recrystallization. This procedure, initially employed in the preparation of mono-[(phosphine)gold(I) chlorides],<sup>20</sup> has been expanded to the synthesis of bis[(phosphine)gold(I) chlorides]<sup>1</sup> and affords several advantages, such as product isolation, over more traditional routes to gold(I) complexes, which involve reduction of Au(III) to Au(I) by excess phosphine ligand and subsequent formation of unwanted phosphine oxide.<sup>21</sup>

The 250-MHz <sup>1</sup>H NMR spectrum of the gold complex **2** showed three peaks in a ratio of 1:1:5, each shifted a fraction of a ppm downfield from a similar display in the <sup>1</sup>H NMR spectrum of Fdpp (see Experimental Section). The 145.8-MHz proton-decoupled <sup>31</sup>P NMR spectrum of **2** in CDCl<sub>3</sub> showed a sharp singlet at 27.39 ppm downfield from the external standard (C-H<sub>3</sub>O)<sub>3</sub>PO. This is a considerable shift from that of the ligand Fdpp (**1**), which showed a single <sup>31</sup>P resonance upfield from the standard at -17.34 ppm. These spectroscopic observations are consistent with the assigned bis(chlorogold) structure **2**,  $\text{Fdpp}(\text{AuCl})_2$ .

The gold-197 Mössbauer spectrum of **2** (Figure 1) provides additional evidence for the assigned structure. The spectrum of **2** is a quadrupole-split doublet indicative of an electric field gradient at the nucleus, usually associated with a center of less than cubic symmetry and consistent with the proposed structure. The isomer shift of 3.81 mm/s relative to gold metal is within the range expected for linearly two-coordinate (phosphine)gold(I) chlorides<sup>22</sup> and is near to that reported for (C<sub>6</sub>H<sub>5</sub>)<sub>3</sub>PAuCl (**3**) of 4.05 mm/s.<sup>23</sup> The quadrupole splitting of 6.93 mm/s is somewhat smaller than the value observed for **3** of 7.52 mm/s. It is difficult to propose a reason for this difference without further study of analogous compounds. The <sup>197</sup>Au Mössbauer spectral parameters are consistent with the absence of significant gold-gold or gold-

- (20) Sutton, B. M.; McGusty, E.; Walz, D. T.; DiMartino, M. J. *J. Med. Chem.* **1974**, *17*, 139.  
 (21) Carloti, F.; Naldini, L.; Simonetta, G.; Malatesto, Q. *Inorg. Chim. Acta* **1967**, *1*, 315.  
 (22) Parish, R. V. *Gold Bull.* **1982**, *15*, 51.  
 (23) Jones, P. G.; Maddock, A. G.; Mays, M. J.; Muir, M. M.; Williams, A. F. *J. Chem. Soc., Dalton Trans.* **1977**, 1434.

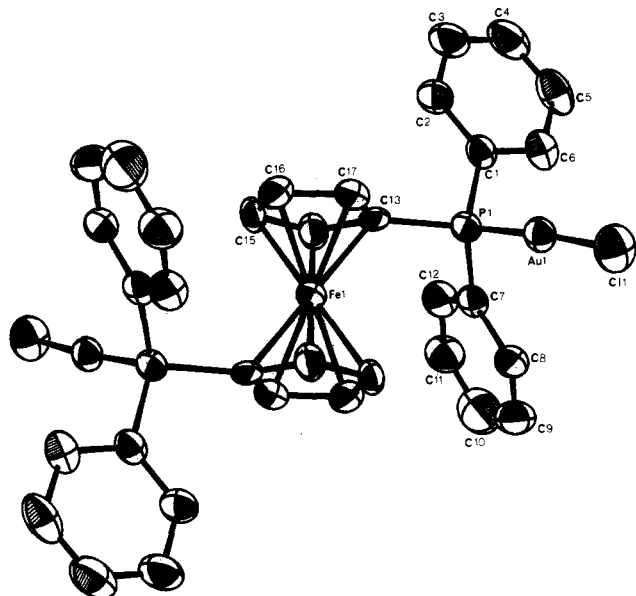


**Figure 3.** View of one of the two crystallographically independent molecules (A) of  $\text{Fdpp}(\text{AuCl})_2$  (**2**). Thermal ellipsoids are drawn at the 50% probability level. Atom Fe1 sits on an inversion center. Unlabeled atoms are related by the symmetry operation to labeled atoms. Hydrogen atoms have been omitted.

iron interactions within the sensitivity of the Mössbauer experiment. The former is noteworthy because of the proximity of atoms Au1 and Au3 (see below). However, a similar observation has been made in the  $^{197}\text{Au}$  Mössbauer spectrum of the large-ring digold complex,  $[\text{Et}_2\text{P}(\text{CH}_2)_2\text{SAu}][\text{AuS}(\text{CH}_2)_2\text{PET}_2]$ , where, despite the Au–Au distance of 3.10 Å, the IS and QS parameters are similar to those for open-chain P–Au–S complexes,<sup>18</sup> indicating little gold–gold interaction. The lack of gold–iron interaction is further confirmed by the iron-57 Mössbauer spectrum of **2** (Figure 2), whose parameters (quadrupole splitting 2.33 mm/s, isomer shift relative to Fe(0) 0.50 mm/s) are very close to those of pristine ferrocene (QS = 2.40 mm/s, IS = 0.47 mm/s).<sup>24</sup> The structure of **2** assigned initially on the basis of the spectroscopic data was confirmed by X-ray crystal structure determination.

There are two crystallographically independent molecules in the structure of **2**. The iron atom of one of these molecules (A) sits on a crystallographic inversion center; thus, the unique portion of this molecule is only half of the formula unit. A second molecule (B) occupies a completely general position within the cell. These molecules are displayed in Figures 3 and 4, respectively. A chloroform solvate molecule also was found; it occupies a general position; thus, there are two  $\text{CHCl}_3$  molecules per unit cell.

Principal bond lengths and angles for both gold-containing molecules are listed in Table III. The Au–P and Au–Cl bond distances fall within normal ranges.<sup>25</sup> The average Fe–C distances are 2.04 (1) Å for molecule A and 2.06 (1) Å for molecule B. The  $\text{C}_{\text{ring}}\text{--C}_{\text{ring}}$  distances average 1.44 (2) Å in all three independent  $\text{C}_5\text{H}_4$  rings.

The geometry about each independent gold atom is linear, two-coordinate, with slight deviations from 180° bond angles at each gold atom. As may be seen from the figures, the two molecules are grossly similar in structure. The most overt difference lies in the rotation of the phosphocyclopentadiene rings relative to one another. Thus, for A, the phosphorous atoms (i.e., the P–Fe–P angle) are exactly 180° opposed and the CP rings are exactly staggered as required by the inversion site symmetry. In molecule B, however, the phosphorous atoms are approximately 150° apart and the CP rings are partially staggered relative to one another. There is a short intermolecular gold–gold contact of 3.083 (1) Å between atoms Au1 and Au3. This short distance

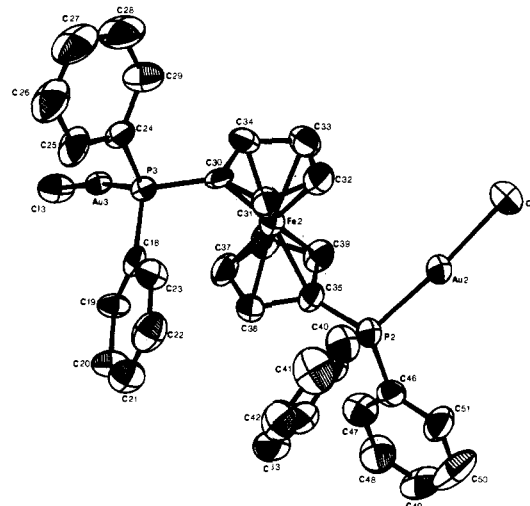


**Figure 4.** View of the second (B) molecule of  $\text{Fdpp}(\text{AuCl})_2$  (**2**). Thermal ellipsoids are drawn at the 50% probability level. Hydrogen atoms have been omitted. Atom Fe2 sits at a general position.

may be indicative of bonding interactions that stabilize the structure in the form of polymeric chains.<sup>26</sup>

**Biological Data.** The ligand **1** and the bis(gold(I)) complex (**2**) were tested for their antitumor activity in mice bearing ip P388 leukemia by following a published procedure.<sup>1</sup> P388 leukemia cells ( $10^6$ ) were inoculated ip in B6D2F<sub>1</sub> mice. Twenty-four hours later, if the tumor inoculum proved to be free of bacterial contamination, animals were randomized into groups of six. Formulations of **1** and **2** in *N,N*-dimethylacetamide and saline were prepared immediately prior to injection<sup>1</sup> and were administered ip on days 1–5 (i.e., treatment was initiated 24 h after tumor inoculation) at five logarithmically spaced dosage levels to identify the maximally tolerated dose (MTD) and the level of antitumor activity produced at this dose. Each experiment included three groups of six animals as untreated controls and animals treated with a positive control, cisplatin (**6**), at two dose levels. Animals were monitored daily for mortality, and experiments were terminated after 45 days. The end point was median survival time (MST) and increase in life span (ILS), which is the percentage of increase in MST relative to untreated controls. Untreated controls inoculated ip with  $10^6$  P388 leukemia cells generally survived for a median of 9–11 days.

The data from **1** and **2** were compared with results obtained from dppe (**4**) and  $\text{dppe}(\text{AuCl})_2$  (**5**), which were included in most experiments as standards together with cisplatin (**6**). The compounds were evaluated in at least two independent dose–response studies to obtain an accurate estimate of the MTD and the extent and reproducibility of the antitumor effect.

The ligand Fdpp (**1**) showed a 30% ILS at an MTD of 231  $\mu\text{mol kg}^{-1} \text{day}^{-1}$ , while the bis(chlorogold) complex **2** showed a 40% ILS at a considerably lower MTD of 4  $\mu\text{mol kg}^{-1} \text{day}^{-1}$ . The lower MTD value for **2** provides an additional example of the increased potency of the gold complex compared to the ligand (**1**) (see Introduction). A similar pattern was observed with dppe (**4**) and  $\text{dppe}(\text{AuCl})_2$  (**5**), which had ILS values of 107% at 50  $\mu\text{mol/kg}$  and 98% at 7  $\mu\text{mol/kg}$ , respectively. However, **4** and **5** were significantly more active than **1** and **2**, essentially doubling the life span of treated animals compared to untreated controls.<sup>1</sup> Cisplatin at an MTD of 2 mg  $\text{kg}^{-1} \text{day}^{-1}$  (6.6  $\mu\text{mol/kg}$ ) produced an average ILS of  $125 \pm 38\%$  in numerous experiments.

**Biological Mechanism.** The mechanism of the antitumor activity of  $\text{dppe}(\text{AuCl})_2$  (**5**) remains speculative but may be attributed to its ability to produce DNA lesions upon displacement of the chlorides<sup>27</sup> in a manner similar to that described for

(24) Collins, R. L. *J. Chem. Phys.* **1965**, *43*, 1072.

(25) Jones, P. G. *Acta Crystallogr.* **1980**, *1336*, 2775. Jones, P. G. *Gold Bull.* **1981**, *14*, 102.

(26) Cooper, M. K.; Mitchell, L. E.; Henciek, K.; McPartlin, M.; Scott, A. *Inorg. Chim. Acta* **1984**, *B4*, L9. Jiang, Y.; Alvarez, S.; Hoffmann, R. *Inorg. Chem.* **1985**, *24*, 749.

(27) Eggleston, D. S.; Chodosh, D. F.; Girard, G. R.; Hill, D. T. *Inorg. Chim. Acta* **1985**, *108*, 221.

dppe[AuSglucose(OAc)<sub>4</sub>]<sub>2</sub> (**6**).<sup>2</sup> The X-ray crystal structure determination of several pseudopolymorphic forms of **5** suggests that there is freedom of rotation about the ethane bridge, allowing the molecule to adopt a range of conformations.<sup>27</sup> A similar situation should exist for **2**, and indeed the X-ray crystal structure determination of **2** shows two distinct forms arising from rotation about the Fe axis. Nevertheless, despite the apparent conformational flexibility and the presence of the two labile chloride ligands, **2** has considerably less antitumor activity than **5**. This loss of activity could be due to the size of the ferrocene spacer that connects the (phosphine)gold moieties. Indeed, the intramolecular Au-Au distance of **2** has been shown to be greater than that of dppe(AuCl)<sub>2</sub> (**5**).<sup>27</sup>

Spacers larger than ethane have been observed to result in loss of activity.<sup>1</sup> Lastly, it has been argued that the cytostatic properties of ferrocene derivatives are due not to the ferrocene moiety itself but rather to the organic residues attached to the rings.<sup>4</sup> The antitumor activity of ferrocenium salts has been ascribed to their dual lipophilic and hydrophilic properties, which allows for ready distribution of the complexes into the aqueous compartments of the affected organisms.<sup>4</sup> The complex **2** does not have saltlike character and is not water soluble. Together, with the larger

spatial separation of the phosphines compared to **5**, these structural and physical property differences may account for the low antitumor activity of **2** in the assays in which it has been tested.

**Acknowledgment.** We thank Edie Reich of the Physical and Structural Chemistry Department and Priscilla Offen of the Analytical Chemistry Department of Smith Kline & French Laboratories (SKF) for the elemental analysis and <sup>31</sup>P NMR spectra, respectively. We also thank Dr. Judith Hempel of SKF for helpful discussion. This work was supported in part by a grant from the Solid State Chemistry Program of the National Science Foundation (NSF Solid State Chemistry Grant No. DMR 8313710) to the Department of Chemistry, Northeastern University.

**Registry No.** **1**, 12150-46-8; **2**, 122092-52-8; **4**, 1663-45-2; **5**, 18024-34-5; **6**, 15663-27-1; <sup>197</sup>Au, 7440-57-5; <sup>57</sup>Fe, 14762-69-7; thiodiglycol, 111-48-8; chlorauric acid, 16903-35-8.

**Supplementary Material Available:** Tables SI-SIII, containing general and anisotropic parameter expressions, bond distances, bond angles, and positional parameters (11 pages); Table SIV, listing observed and calculated structure factors (68 pages). Ordering information is given on any current masthead page.

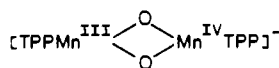
Contribution from the Laboratoire de Chimie Bioorganique et Bioinorganique, URA CNRS 1384, Institut de Chimie Moléculaire d'Orsay, Université Paris-Sud, 91405 Orsay, France, Laboratoire de Chimie Inorganique, URA CNRS 420, Institut de Chimie Moléculaire d'Orsay, Université Paris-Sud, 91405 Orsay, France, Laboratoire de Biochimie, Hôpital Raymond Poincaré, 92380 Garches, France, and Laboratoire de Pharmacochimie, UER de Médecine et de Pharmacie, 76800 Saint-Etienne du Rouvray, France

## Voltamperometric and Spectroscopic Studies of the Behavior of Manganese(II) and Manganese(III) Porphyrins with Dioxygen and Superoxide. Evidence for the Formation of a Mixed-Valence Dimeric Manganese Porphyrin

M. Perrée-Fauvet,\*† A. Gaudemer,† J. Bonvoisin,‡ J. J. Girerd,‡ C. Boucly-Goester,§ and P. Boucly||

Received December 31, 1988

The reactions of superoxide ion with Mn<sup>II</sup>TPP(py) and Mn<sup>III</sup>TPP<sup>+</sup> have been studied by linear voltammetry, visible spectroscopy, and EPR spectroscopy. Depending on the concentration of superoxide ion, two complexes of very comparable thermodynamic stabilities are generated. The first one, presumably [MnTPPO<sub>2</sub>]<sup>-</sup>, results from the stoichiometric 1/1 addition of O<sub>2</sub><sup>-</sup> to Mn<sup>II</sup>TPP(py). It can undergo a one-electron reduction at a very negative potential and is EPR silent. The second one, which can be reduced by two electrons at the same potential, is obtained by adding 0.5 equiv of O<sub>2</sub><sup>-</sup> to Mn<sup>II</sup>TPP(py) or by addition of an excess of O<sub>2</sub><sup>-</sup> to Mn<sup>III</sup>TPP<sup>+</sup>. It exhibits a 16-line EPR spectrum, which is typical of a mixed-valence dimeric manganese complex. Hyperfine constants of 81 and 163 G were obtained by simulation. Magnetic susceptibility measurements and EPR analysis are in agreement with a strongly antiferromagnetically coupled Mn(III)/Mn(IV) dimer. To take into account the reducing conditions under which it is generated and the very low reduction potential value, we propose the following anionic structure:



### Introduction

Manganese porphyrins have proved to be efficient catalysts in the oxidation of olefins with single oxygen atom donors such as iodosylbenzene,<sup>1</sup> alkyl hydroperoxides,<sup>2</sup> amine *N*-oxides,<sup>3</sup> hypochlorites,<sup>4</sup> hydrogen peroxide,<sup>5</sup> periodate,<sup>6</sup> and persulfate.<sup>7</sup> An oxomanganese(V) porphyrin has been postulated as the intermediate active species. The oxidation reactions by molecular dioxygen catalyzed by manganese porphyrins are less efficient, because they require the presence of a reducing agent: borohydride,<sup>8</sup> H<sub>2</sub>/Pt,<sup>9</sup> ascorbate,<sup>10</sup> *N*-methylidihydronicotinamide,<sup>11</sup> Zn,<sup>12</sup> or electrochemical reduction.<sup>13</sup>

We have recently found,<sup>14</sup> that the systems manganese(III) porphyrin/reducing agent/dioxygen and manganese(III) por-

phyrin/superoxide ion both catalyze the oxidation of 2,4,6-*tert*-butylphenol and lead to the same oxidation products, whereas

- (1) (a) Groves, J. T.; Kruper, W. J.; Haushalter, R. C. *J. Am. Chem. Soc.* **1980**, *102*, 6375. (b) Hill, C. L.; Schardt, B. C. *Ibid.* **1980**, *102*, 6374. (c) Smegal, J. A.; Hill, C. L. *J. Am. Chem. Soc.* **1983**, *105*, 2920. (d) Mansuy, D.; Leclaire, J.; Fontecave, M.; Dansette, P. *Tetrahedron* **1984**, *40*, 2847. (e) Lindsay Smith, J. R.; Mortimer, D. N. *J. Chem. Soc., Perkin Trans. 2* **1986**, 1743.
- (2) (a) Mansuy, D.; Battioni, P.; Renaud, J. P. *J. Chem. Soc., Chem. Commun.* **1984**, 1255. (b) Balasubramanian, P. N.; Sinha, A.; Bruice, T. C. *J. Am. Chem. Soc.* **1987**, *109*, 1456.
- (3) (a) Powell, M. F.; Pai, E. F.; Bruice, T. C. *J. Am. Chem. Soc.* **1984**, *106*, 3277. (b) Wong, W. H.; Ostovic, D.; Bruice, T. C. *J. Am. Chem. Soc.* **1987**, *109*, 3428.
- (4) (a) Meunier, B.; Guilmet, E.; De Carvalho, M. E.; Poilblanc, R. *J. Am. Chem. Soc.* **1984**, *106*, 6668. (b) De Poorter, B.; Meunier, B. *J. Chem. Soc., Perkin Trans. 2* **1985**, 1735. (c) Razenberg, J. A. S. J.; Nolte, R. J. M.; Drenth, W. *Tetrahedron Lett.* **1984**, *25*, 789; *J. Chem. Soc., Chem. Commun.* **1986**, 277.
- (5) Renaud, J. P.; Battioni, P.; Bartoli, J. F.; Mansuy, D. *J. Chem. Soc., Chem. Commun.* **1985**, 888.
- (6) Takata, T.; Ando, W. *Tetrahedron Lett.* **1983**, *24*, 3631.

\* Laboratoire de Chimie Bioorganique et Bioinorganique, Université Paris-Sud.

† Laboratoire de Chimie Inorganique, Université Paris-Sud.

‡ Hôpital Raymond Poincaré.

§ UER de Médecine et de Pharmacie.